REPORT DOCUMENTATION PAGE

Form Approved
OMB No. 0704-0188

1. REPORT DATE *(DD-MM-YYYY)*	2. REPORT TYPE	3. DATES COVERED *(From - To)*
	Technical Papers	

4. TITLE AND SUBTITLE

Please see attached

5a. CONTRACT NUMBER

5b. GRANT NUMBER

5c. PROGRAM ELEMENT NUMBER

6. AUTHOR(S)

5d. PROJECT NUMBER
2308

5e. TASK NUMBER
M19B

5f. WORK UNIT NUMBER
346058

7. PERFORMING ORGANIZATION NAME(S) AND ADDRESS(ES)

Air Force Research Laboratory (AFMC)
AFRL/PRS
5 Pollux Drive
Edwards AFB CA 93524-7048

8. PERFORMING ORGANIZATION REPORT

9. SPONSORING / MONITORING AGENCY NAME(S) AND ADDRESS(ES)

Air Force Research Laboratory (AFMC)
AFRL/PRS
5 Pollux Drive
Edwards AFB CA 93524-7048

10. SPONSOR/MONITOR'S ACRONYM(S)

11. SPONSOR/MONITOR'S NUMBER(S)

Please see attached

12. DISTRIBUTION / AVAILABILITY STATEMENT

Approved for public release; distribution unlimited.

13. SUPPLEMENTARY NOTES

14. ABSTRACT

20030205 292

15. SUBJECT TERMS

16. SECURITY CLASSIFICATION OF:			17. LIMITATION OF ABSTRACT	18. NUMBER OF PAGES	19a. NAME OF RESPONSIBLE PERSON
			A		Leilani Richardson
a. REPORT	**b. ABSTRACT**	**c. THIS PAGE**			**19b. TELEPHONE NUMBER** *(include area code)*
Unclassified	Unclassified	Unclassified			(661) 275-5015

Standard Form 298 (Rev. 8-98)
Prescribed by ANSI Std. 239.18

MEMORANDUM FOR PRS (In-House Publication)

FROM: PROI (STINFO)   16 Apr 2001

SUBJECT: Authorization for Release of Technical Information, Control Number: **AFRL-PR-ED-TP-2001-088**
  Ingrid Wysong, Rainer Dressler, Iain Boyd, "Evaluation of DSMC Dissociation Models through
  Comparison to Measured Cross Sections"

Journal of Thermophysics and Heat Transfer   (Statement A)
(Deadline: N/A)

1. This request has been reviewed by the Foreign Disclosure Office for: a.) appropriateness of distribution statement,
b.) military/national critical technology, c.) export controls or distribution restrictions,
d.) appropriateness for release to a foreign nation, and e.) technical sensitivity and/or economic sensitivity.
Comments:_____
_____
_____
_____

Signature _____   Date _____

2. This request has been reviewed by the Public Affairs Office for: a.) appropriateness for public release
and/or b) possible higher headquarters review.
Comments: _____
_____
_____
_____

Signature _____   Date _____

3. This request has been reviewed by the STINFO for: a.) changes if approved as amended,
b) appropriateness of references, if applicable; and c.) format and completion of meeting clearance form if required
Comments:_____
_____
_____

Signature _____   Date _____

4. This request has been reviewed by PR for: a.) technical accuracy, b.) appropriateness for audience, c.)
appropriateness of distribution statement, d.) technical sensitivity and economic sensitivity, e.) military/
national critical technology, and f.) data rights and patentability
Comments:_____
_____

APPROVED/APPROVED AS AMENDED/DISAPPROVED

PHILIP A. KESSEL   Date
Technical Advisor
Space and Missile Propulsion Division

EVALUATION OF DSMC DISSOCIATION MODELS THROUGH COMPARISON TO MEASURED CROSS SECTIONS

Ingrid J. Wysong[*]
Air Force Research Laboratory, Propulsion Directorate
Edwards AFB, CA 93524

Rainer A. Dressler,[†] Y.H. Chiu[‡]
Air Force Research Laboratory, Space Vehicles Directorate
Hanscom AFB, MA 01731

Iain D. Boyd[§]
Department of Aerospace Engineering
University of Michigan, Ann Arbor, MI 48109

Abstract

Recent measurements of collision-induced dissociation (CID) cross sections for Ar_2^+–Ar collisions for vibrationally cold and hot cases are utilized to test and compare several CID models that have been proposed for the direct simulation Monte Carlo (DSMC) technique. The idea that the CID process is strongly favored by vibrational energy is discussed relative to the various models. The Ar_2^+ data do not show any vibrational favoring of the CID cross sections. It is shown that some DSMC CID models have much more physically realistic behavior in terms of their cross sections than others.

Nomenclature

A	Scaling parameter for cross sections
A'	Arrhenius parameter
D	Dissociation energy
E_a	Activation or threshold energy
E_c	Collision energy
E_i	Internal energy
E_{tr}	Translational energy
f_v	Fraction of energy in vibrational mode
h	Planck's constant
k	Thermal reaction rate coefficient
k_v	Vibrational-state-specific reaction rate coefficient
n	Scaling exponent for cross sections
N_v	Boltzmann fraction of population in level v
P	Probability of dissociation
v	Vibrational quantum number
ζ	Degrees of freedom
η	Arrhenius parameter, temperature exponent
λ	Vibrational favoring parameter

[*] Senior Scientist, Aerophysics Branch. Senior Member, AIAA; ingrid.wysong@edwards.af.mil
[†] Senior Scientist, Space Vehicles Directorate. Member AIAA
[‡] Boston College, Institute for Scientific Research
[§] Associate Professor, Aerospace Engineering. Member AIAA

σ°	Prior cross section
σ_R	Cross section for CID reaction
σ_{tot}	Total collision cross section
σ_{ref}	Reference cross section (VHS parameter)
ν	Photon frequency
ϕ	Vibrational favoring parameter
ω	VHS parameter

Introduction

The direct simulation Monte Carlo (DSMC) method is now widely utilized for prediction of rarefied gas flowfields; however, validated dissociation and other chemical reaction models continue to be needed for the case of reacting gases. The total collision energy model is most often used, where the probability of reaction for a given collision is a function of the total collision energy in a way that reproduces a given equilibrium rate coefficient over a range of temperatures.[1] It has been widely accepted for some time that in the case of diatomic dissociation reactions, the probability of reaction is enhanced for higher vibrational levels for a given collision energy. Thus, the need has been recognized for a DSMC dissociation model that includes this vibrational favoring effect, yet retains computational efficiency. The details of the DSMC dissociation model have been shown to have a large effect on predictions of reacting flowfields where the internal energy distribution is far from equilibrium.[2,3]

Several previous studies have attempted to address the need for an improved DSMC dissociation model.[4,5,6,7,8,9,10,11] These studies have been hampered, however, by a dearth of experimentally measured, state-specific cross section data. They have generally made comparisons, instead, with shock tube measurements of high-temperature nonequilibrium dissociation rate coefficients (where the governing vibrational populations are not well defined) and dissociation induction time. In addition, some comparisons have been made with calculated state-specific rate coefficients from quasi-classical trajectory studies.[5]

Much of the existing chemical physics literature on dissociation of small molecules (both measurements and calculations) provides information in the form of rate coefficients. Rate coefficients inherently assume either full equilibrium or at least translational equilibrium at some temperature. The physics of individual collisions, however, is described by cross sections for processes as a function of translational energy, internal quantum states of the reactants and products, angular scattering distributions, etc. DSMC can potentially reproduce reacting flowfields under conditions that are far from equilibrium

2

(even translational equilibrium), but the technique requires incorporation of physically realistic cross sections.

Measured cross sections for collision-induced dissociation (CID) of neutral diatomics are almost unknown. As discussed below, CID cross section measurements for ionic species are quite common and provide detailed information on dissociation threshold energies. A recent review is provided by Armentrout[12]. However, data on the effect of vibrational excitation on CID of diatomics have been very limited. Most of the existing work has involved the vibrational energy dependence of H_2^+ collision-induced dissociation.[13,14] Large vibrational enhancements were observed for this molecule, for which large quantum effects may be expected. The present Ar_2^+ data are extremely valuable as the first measurement of dissociation cross sections including the effect of vibrational excitation for a heavier, more classical molecule.[15]

The goal of this paper is to utilize the recently published CID cross sections for Ar_2^+–Ar collisions for vibrationally cold and hot conditions to test some of the CID models that have been proposed for DSMC and a well-known model frequently used in the chemical physics literature. Since the majority of these models have been formulated in terms of matching given equilibrium rate coefficients, the emphasis here on examining the cross sections themselves will allow some new perspective. In addition, the Ar_2^+ data will provide a "reality check" for a particular CID case for the types of vibrational favoring that have been proposed in the models. Finally, the opportunity will be taken to discuss the role of the total collision cross section in the DSMC chemistry model.

Vibrational Favoring

Levine and Manz[16] have addressed the fact that many atom exchange reactions show a much-greater-than-statistical vibrational excitation in the products. They have shown that the principle of detailed balance requires that those reactions that produce enhanced post-reaction vibrational excitation in the exoergic direction must also have their reaction probability enhanced by vibrational excitation of reactants in the reverse (endoergic) direction. We will refer to this characteristic as "vibrational favoring." Note that any endoergic reaction will be enhanced by vibrational excitation, merely because the amount of total energy available in the collision is increased (assuming that all types of energy contribute to overcoming

3

the activation energy). "Vibrational favoring" refers to the vibrational energy being more effective than other types of energy in promoting reaction.

While CID reactions of diatomic molecules are often considered to be vibrationally favored, unambiguous information on the degree of favoring has so far been quite limited. The dissociation reactions of both H_2 and its ion, H_2^+, have been shown by an extensive body of work to be strongly vibrationally favored. Results on these molecules include measured[13,14] and calculated[17] state-specific dissociation cross sections and calculated state-specific rate coefficients.[18] Hydrogen, however, is not considered a typical diatomic molecule in most respects, due to its large vibrational and rotational level spacings. Unfortunately, no state-specific dissociation measurements are yet available for O_2 or N_2. Instead, some shock tube data on the quasisteady nonequilibrium dissociation rate coefficient and incubation time have been obtained for these species and for Br_2 and I_2, and a number of studies have attempted to deduce information on the degree of vibrational favoring based on these macroscopic quantities. Thorough analysis of these data based on models for state-specific dissociation and vibrational relaxation rate coefficients indicates that there is some degree of vibrational favoring in the state-specific rate coefficients (see, for example: Marrone and Treanor,[19] Kiefer and Hajduk,[20] Sergievskaya et al.[21]). In addition, recent quasi-classical trajectory (QCT) calculations[22] for N_2-N CID indicate that this reaction is vibrationally favored,[23] as do preliminary QCT results for O_2-Ar.[24]

Summary of Experiment

Perhaps the best experimental data available on the translational and vibrational energy dependence of CID cross sections have been obtained in ion beam experiments. Neutral beam studies also exist for systems where ionic dissociation limits are observed, making product detection efficient.[25] Ion beam experiments afford straight-forward translational energy control, and state-selected beams can be produced using various photoionization techniques. Chupka et al.[14] measured the translational energy dependence of $H_2^+(X, v = 0-5)$ + He CID cross sections. Govers and Guyon[26] later conducted a more detailed study of $H_2^+(X, v = 0-6)$ + He CID at a single collision energy of 3.1 eV including cross sections and product ion recoil velocity analysis. Large degrees of vibrational favoring were observed in both experiments. The experimental cross sections near threshold, however, were affected by large-angle scattering collection efficiency problems. Liao et al.[13] exploited the guided-ion beam technique to overcome collection

4

efficiency problems and investigated $H_2^+(X, v = 0\text{-}4) + Ar$ CID cross sections. Here again, large vibrational effects were observed. Franck-Condon constraints associated with the applied photoionization techniques limited the experiments to low vibrational levels of the reactants. No state-selected CID studies exist at vibrational levels approaching the dissociation limit.

Recently, Chiu et al.[15] devised an experiment in which diatomic ions are formed in the nonequilibrium conditions of a supersonic jet, thereby providing access to a broader range of vibrational levels compared with previous photoionization techniques. A brief summary of their experimental technique described in detail in their paper is provided in the following. Figure 1 is a schematic view of the supersonic jet ion source. Two magnetically confined, counter-propagating electron beams cross a supersonic jet emanating from a translatable pulsed valve (nozzle diameter 0.5 mm). The valve translation allows variation of the distance between the nozzle and the point of ionization. In a first experiment, Chiu et al. generated Ar_2^+ ions by using argon gas at a stagnation pressure of ~3.5 atm. Ar_2^+ is formed through 3-body association reactions,

$$Ar^+ + 2\, Ar \rightarrow Ar_2^+ + Ar, \tag{1}$$

or from direction ionization and subsequent evaporation of neutral trimers or larger clusters. Subsequent bimolecular collisions cool the dimer ions, while additional 3-body collisions can form larger cluster ions. The latter can evaporatively cool to form Ar_2^+ again. By extending the distance between the ionization point and the nozzle, the number of collisions following ionization is reduced, thus leading to inefficiently relaxed ions. The valve position thus controls the internal energy of the dimer ions. Since rotational cooling in supersonic jets is very efficient, it is safe to assume that the investigated diatomic ions are rotationally cold. The internal energy of the ions is, therefore, vibrational and/or electronic.

The jet ions are mass selected and decelerated prior to injection into an ion guide consisting of two rf octopoles in series. The first octopole guides the mass selected Ar_2^+ through a collision cell containing the Ar target gas. Primary Ar_2^+ ions and secondary Ar^+ dissociation product ions are radially confined by the octopole rf field and are extracted from the second octopole at the entrance of a quadrupole mass analyzer. Following mass analysis, the ions are detected with a microchannel plate electron multiplier. CID cross sections are obtained from the measured primary and secondary ion currents and the target cell density that is measured using a capacitance manometer. The primary ion beam pulses can be narrowed down to ~3 μs,

5

and product recoil velocity distributions can be measured by recording the arrival times of CID fragment ions, Ar$^+$. The velocity transformed time-of-flight (TOF) spectra represent the axial velocity component of the recoil velocities.

In parallel with the CID measurements, the internal energy of the reactant ions is determined using a photodissociation scheme:

$$Ar_2^+ + h\nu \rightarrow Ar^+ + Ar + E_{tr},$$ (2)

where $h\nu$ is the photon energy and E_{tr} is the kinetic energy of the photofragments. The photodissociation kinetic energy release is determined by measuring the recoil velocity distributions of the photofragment ions as described by Williams et al.[27] In the photodissociation experiment, a tunable, pulsed laser beam intersects the Ar$_2^+$ ion pulses in the second octopole ion guide, and photofragment ion arrival times are recorded. Velocity transformed TOF spectra are modeled to provide the kinetic energy release distributions, $f(E_{tr})$. The corresponding internal energy E_i, is given by:

$$E_i = E_{tr} + D + E_{so} - h\nu$$ (3)

where D is the dissociation energy of Ar$_2^+$ and E_{so} is the spin orbit splitting of Ar$^+$ (^2P_J). The internal energy distribution is then given by:

$$f(I_i) = f(E_{tr})g(E_{tr})$$ (4)

where $g(E_{tr})$ is a correction factor given by the corresponding photodissociation Franck-Condon factor. One reason for choosing Ar$_2^+$ in this case study is the accurately known dissociation energy, $D = 1.3144 \pm 0.0007$ eV, as determined spectroscopically by Signorell et al.[28] The inclusion of $E_{so} = 0.178$ eV in Eq. (3) is mandated by the photodissociation mechanism involving the UV-VIS $^2\Sigma_g^+ \leftarrow ^2\Sigma_u^+$ transition in Ar$_2^+$. The $^2\Sigma_g^+$ excited state dissociates to the spin-orbit excited asymptote, Ar$^+$($^2P_{1/2}$) + Ar.

Experiments were carried out at three ionization point – nozzle distances, 0.5, 3 and 5 mm. In their original work, Chui et al. concluded that the measurements at 5 mm were affected by electronically metastable Ar$_2^+$ ions for which the photodissociation probe was not sensitive. The present work concentrates only on the measurements at 0.5 and 3 mm. The CID cross sections are shown in Figure 2. The cross sections are observed to increase rapidly with energy above a certain threshold, after which a

6

plateau is reached. While the 0.5 mm measurement, referred to as "cold," exhibits an onset near the thermochemical threshold of 1.31 eV, the measurements at 3 mm, referred to as "hot," are clearly shifted to lower collision energies, implying internal excitation of the ions. A nonlinear least squares fit of the modified line-of-centers cross section (LCCS) model, attributed to Rebick and Levine discussed in more detail below,

$$\sigma^o = A \frac{\left(E_c - E_a\right)^n}{E_{tr}} \qquad (5)$$

to the cold data including a convolution of the experimental translational energy distribution, yields $A = 14.43$, $E_a = 1.34 \pm 0.10$ eV, and $n = 1.23$. Here, E_a is the activation energy for the reaction, E_{tr} is the translational energy, $E_c = E_{tr} + E_i$ is the collision energy and E_i is the internal energy. The fit result is shown as a dashed curve. Note, that the fit is only carried out in the growth part of the curve. In concert with the LCCS model, the plateau may be regarded as an effective hard-sphere cross section.

The threshold of 1.34 ± 0.10 eV is within experimental error equal to the dissociation energy, and it can be concluded that internal excitation of the cold ions is minimal. The low-energy pre-threshold signal is attributed to small amounts of metastables in the ion beam. A similar fit to the hot data yields a threshold of 0.76 ± 0.15 eV indicating an average internal energy of 0.55 ± 0.15 eV for the assumption that A and n do not change with internal excitation.

Figure 3 displays the internal energy distributions as obtained from the photodissociation experiments and associated analysis. The width of the cold distribution lies close to the statistical accuracy of the fitting algorithm at the particular experimental conditions (355 nm photoexcitation). The hot distribution peaks at 0.5 eV and exhibits a shoulder at higher energies. The distribution corresponds to an average internal energy of 0.77 ± 0.10 eV. Note that this value is higher than that estimated from fitting the hot distribution to a threshold function with A and n parameters determined for ions assuming no vibrational favoring. This signifies that vibration may in fact be inhibitive. An estimate based on Rebick and Levine's surprisal analysis (see Eq. (6) in subsequent section) determines a λ parameter of 1. Given the substantial sources of errors in the photodissociation analysis, particularly for very high and low vibrational levels (the Franck-Condon factors at 630 nm favor the states in the center of the distribution), it is more safe to state that there is little evidence for vibrational favoring in the present system.

7

The CID product recoil velocity distribution measurements[15] are revealing with respect to the detailed CID mechanism. The laboratory axial velocity distributions are near-symmetric with respect to the center-of-mass velocity during the cross section growth collision energy range, and become distinctly forward scattered at higher energies where the cross section becomes more or less independent of energy. The near isotropic scattering at energies near threshold is indicative of low-impact parameter collisions associated with efficient energy transfer. Such collisions can be described to involve statistical energy partitioning in the collision complex. The forward-scattering implies larger impact parameter collisions involving less efficient energy transfer. Such events normally involve direct dynamics, such as an atom stripping mechanism.

The measurements are consistent with Ar_3^+ potentials calculated by De Lara *et al.*[29] Examples of the potential seams are shown in Figure 4. Ar_3^+ can be regarded as having an Ar_2^+ core with a loosely bound Ar atom. This is expressed by the very weak $Ar-Ar_2^+$ chemical bond when the Ar_2^+ moiety bond length is at its equilibrium distance of 4.69 au (1 au = 0.529 Å). From the onset of the repulsive interaction averaged over all orientation angles, θ, the potentials yield a hard-sphere cross section of ~45 Å^2. This is about a factor of 3 larger than the plateau cross sections observed in the CID experiments. A very similar magnitude of effective hard-sphere cross section was observed by Parks *et al.* in CsI + Rg CID studies.[25] The figure also demonstrates that slight stretching of the bond results in a substantially higher attractive interaction in the collinear approach. This may contribute to the larger effective hard-sphere cross sections for the hot ions.

Total Cross Section

Comparisons with some of the DSMC models will require an assumed form for the total collision cross section, σ_{tot} (note that in this context, total cross section is a transport-type cross section, not the integral elastic cross section). These transport cross sections are used in DSMC to define a value of local collision frequency via the variable hard sphere (VHS)[1] or variable soft sphere (VSS) models,[30] and are thus fundamental to the entire DSMC technique.

VHS and VSS cross sections are based on inverse power-law potential point center of repulsion (or attraction) and have been shown to reproduce flowfields such as shock waves that are sensitive to transport (viscosity, diffusion) as a function of temperature. However, they assume either isotropic scattering (VHS) or non-isotropic scattering that is constrained in such a way as to match a given diffusion coefficient (VSS).

8

Reactions and inelastic collisions are defined as a probability per elastic collision as defined by the transport/momentum transfer cross section. For ion-neutral collisions, very little work has been done on the appropriateness of these models (however, Nanbu and Kitatani have examined a detailed collision model for the case of ions in a parent gas[31]). For Ar_2^+-Ar collisions, the mobility[32] over the measured temperature range (200 – 1300K) is reproduced well by an R^{-4} inverse power law potential, which is not surprising since the induced-dipole attractive force will be dominant in this range ($0.005 < E_c < 0.2$ eV). At higher energies, however, both attractive and repulsive parts will contribute, and at even higher energies, the repulsive wall of the potential will dominate transport. Information on the potential indicates a roughly 10-4 to 12-4 repulsive-attractive form, so we make a very simplified assumption of R^{-10} repulsive behavior (VHS model) for $E > 0.2$eV. This leads to an $\omega = 0.7$ value for the VHS parameter, with $\sigma_{ref} = 54.7$ Å^2 at 0.2 eV based on the mobility data. These values are used below where VHS is indicated. A generalized hard sphere DSMC collision cross section model has been proposed by Hassan and Hash[33] which allows inclusion of the effects of an attractive-repulsive potential, and could be useful for more detailed studies in this collision energy range.

If one were to instead consider only the mobility data and assume that the R^{-4} behavior could be extrapolated to the high end of the collision energy range examined here, that would lead to a VHS parameter of $\omega = 1$, producing $\sigma_{tot} = 10$ A^2 (less than the measured σ_R) at $E_{tr} = 5$ eV instead of the 27 A^2 produced by the $\omega = 0.7$ value. While it is not physically impossible for a given inelastic process to have a cross section which is larger than σ_{tot} (in the present sense of the transport cross section), the DSMC sampling approach is in practical terms limited to processes which have cross sections smaller than σ_{tot}, and may produce undesired results even in the case that σ_R becomes close to σ_{tot}.

Another issue may arise when dealing with molecules that have large amounts of vibrational excitation: does the vibrational stretching of the bond translate into an increase in the total collision cross section, and, if so, how much? The potentials in Figure 4 certainly indicate that the long-range attractive force may increase dramatically with increasing Ar_2^+ bond length. Several studies have attempted to address this question in various ways.[34,35] Further discussion of this point is beyond the scope of the present study, but it is raised as a reminder that any variation in the hard-sphere or total cross section as a function of vibrational state, v, has been neglected in the ensuing analysis. Any variation in the CID cross section

9

for Ar_2^+–Ar collisions that is due to an increase in the total cross section with vibration is neglected in all the models under discussion.

CID Models for DSMC

While it has already been concluded above that the Ar_2^+ dissociation reaction does not show any significant vibrational favoring effect, it is worthwhile to compare the results with several proposed DSMC chemistry models that attempt to include vibrational favoring. The vast majority of previous validation studies have examined rate coefficients only (which, as discussed above, are basically an equilibrium quantity), and some surprising trends may be observed by comparing cross sections rather than rates. It will be seen that, even allowing for the fact that some reactions may have a vibrational favoring effect that Ar_2^+–Ar CID does not show, some of the models exhibit unphysical cross sections or probabilities in certain collision energy ranges.

As discussed in the experimental section, it is expected that the Ar_2^+ produced in a supersonic jet is very cold rotationally, so the following analysis assumes that the rotational energy is zero ($E_r = 0$). For each model we assume that the activation energy $E_a = D = 1.314$ eV. Some of the models are based on reproducing a given rate coefficient. In those cases, some assumption must be made as to the choice of σ_{tot}, and the assumed VHS form of $\sigma_{tot}(E_{tr})$ discussed above is used. For the models that predict a form for the reaction cross section directly, any assumption about σ_{tot} does not enter into the comparison between the model and the measured reaction cross section (σ_R). If implemented in a DSMC code, these model σ_R values would be divided by whatever σ_{tot} value the code is using to obtain a reaction probability for each collision.

While the Ar_2^+ internal energy distribution measurements provide relative populations within certain bins of internal energy, here we treat each bin as a notional "vibrational level," $v = 0$ to 25, of the Ar_2^+ molecule. The table of "vibrational number," vibrational energy, and relative population for the two measured cases is given in Table 1.

The Model of Rebick and Levine

10

This model is the modified LCCS model mentioned above and is due to Rebick and Levine,[36] where a semi-empirical expression for the "prior," or "statistical" case cross section with no vibrational favoring is:

$$\sigma^o = A \frac{\left(E_c - E_a\right)^n}{E_{tr}} \tag{5}$$

for $E_c = E_{tr} + E_i > D$; $\sigma_R = 0$ otherwise. Here, E_a is the activation energy for the reaction, which we will assume is equal to D, E_i is the internal energy and is here equal to the vibrational energy E_v, and n usually takes on values between 1 and 2.5 ($n = 1$ corresponds to LCCS). A is an adjustable constant. It is assumed that the total collision cross section is constant (hard sphere). With vibrational favoring determined by the value of a parameter, λ, the cross section becomes:

$$\sigma(v) = \sigma^o \exp\left(-\lambda f_v\right) =$$
$$A \frac{\left(E_c - E_a\right)^n}{E_{tr}} \exp\left(-\lambda f_v\right) = AP(v, \lambda, E_{tr}) \tag{6}$$

where $f_v = E_v/E_c$. To compare with the measurements, the Rebick - Levine model is computed using:

$$\sigma(E_{tr}) = A \sum_v c_v P(v, \lambda, E_{tr}), \tag{7}$$

where $c(v)$ are the normalized coefficients representing the measured vibrational population as shown in table 1, and A is a scaling parameter that is adjusted to match the experimental data at an arbitrary translational energy of 5 eV.

For the cold case, the value of λ has very little effect on the shape of the cross section. Figure 5(a) shows the predicted cross section for the cold case, all for $\lambda = 0$, for three values of n (the values for A are 19, 10, and 5, respectively). It is seen that a curvature parameter $n = 1.5$ reproduces the shape of the cross section quite well. In Figure 5(b), cross sections for the two measured distributions are computed for $n = 1.5$ and $\lambda = 0$, and -2 (the value for A is 10 for both cases). Note that the primary and target gas velocity distributions cause broadening in the experimental translational energy distributions. This accounts for the minor energy shift between the calculated and measured cold curves.

11

Weak Vibrational Bias (WVB) Model

The weak vibrational bias model (WVB) is Koura's[6] formulation. It is based on combining Kiefer's vibrationally favored state-specific rate coefficient expression[20] with the LCCS model; Kiefer's in turn is closely based on Rebick - Levine. WVB also allows for a variation in total cross section with E_{tr}. The expression is:

$$\sigma_R(v, E_{tr}) = \sigma_{tot} A \left[1 - \frac{(D - E_v)}{E_{tr}} \right] \exp \left[\lambda \left(\frac{E_v}{D} \right) - 1 \right] = A \frac{E_c - D}{E_t} \exp \left[\lambda \left(\frac{E_v}{D} \right) - 1 \right] \tag{8}$$

for $E_c > D$; $\sigma_R = 0$ otherwise. Here, A is again an adjustable constant. The parameter λ controls the vibrational favoring. There is an unfortunate difference in the sign convention between the Rebick - Levine model (and Maximum Entropy model, below), where a negative value indicates vibrational favoring, and the WVB model, where a positive value indicates favoring. For the case of $\lambda = 0$, the probability is the prior LCCS case times the VHS or VSS total cross section, σ_{tot}. Notice that for the prior case, so long as $A \bullet 1$, $P(v)$ is always $\bullet$ 1, which makes the above expression well-behaved for DSMC application. In contrast, the Rebick - Levine prior probability expression will become greater than unity for high E_{tr} when $n > 1$. The Rebick - Levine model for $n = 1$ and $\lambda = 0$ will give identical results to the WVB model for $\lambda = 0$. The models differ, however, in the formulation of the vibrational favoring. Rebick - Levine's is a function of f_v ($= E_v/E_c$), while WVB is a function of E_v/D. The WVB bias formulation, as noted above, follows Kiefer.[20] The Kiefer/WVB formulation appears to be preferable, as the Rebick - Levine formulation leads to a possibly unphysical "bump" in the state-specific cross section when f_v is large (i.e., for high vibrational levels and translational energies near the threshold) and absolute values of λ greater than 2 or so (see Figure 6(a) for $\lambda = -5, -20$). In addition, it can be shown that the validation comparisons made by Rebick and Levine[36] for state-specific dissociation cross section versus collision energy for $H_2^*(v)$ can be equally well reproduced using the Kiefer formulation (in this particular case, the Rebick - Levine formulation roughly fits the experimental results for $v = 0, 3,$ and 5 if $\lambda = -8.3$, while the Kiefer formulation fits the data about equally well for $\lambda = 5$).

Using the WVB Model (Eq. 8) we compute the $Ar_2^+ + Ar$ CID cross sections using the analogous procedure discussed above for the Rebick-Levine model (Eq. 7). The sum is multiplied by the VHS σ_{tot} at each E_{tr} and A is selected such that the calculated cross section at cold vibrational population is equal to the measured value at $E_{tr} = 5$ eV for the cold case. Results are shown in Figure 5(c) for the cases of $\lambda = 0$ and 2 when the total cross section is assumed constant (hard sphere). The values of A are 19 and 110 $Å^2$, respectively. Koura has suggested $\lambda = 2$ for $O_2 -$ Ar CID. Figure 5(d) shows the result for the $\lambda = 0$ case when the total cross section follows the VHS form (now A is 0.66) to demonstrate that there is a substantial effect of the σ_{tot} assumption on the shape of σ_R.

Maximum Entropy Model

The Maximum Entropy (ME) model is due to Gallis and Harvey[7] and Marriott and Harvey.[37] This model is also based on the ideas of Levine, but uses a significantly different formulation. It begins with the statistical probability distribution for depositing a given fraction of E_c into a particular mode (in this case, vibration) after a collision and assumes that this same expression also gives the prior probability for chemical reaction (in this case, dissociation) as a function of the fraction of energy in the vibrational mode. Thus,

$$P^o(f_v) = \frac{\Gamma(\zeta_v + \zeta_b)}{\Gamma(\zeta_v)\Gamma(\zeta_b)} f_v^{\zeta_v - 1}(1 - f_v)^{\zeta_b - 1} \tag{9}$$

where $f_v = E_v / E_c$, ζ_v is the average number of degrees of freedom (DOF) for vibration (in this case, $(2+0)/2 = 1$), ζ_b is the average number of DOF in all other modes (in this case, 0 for rotation plus $(5/2 - \omega)$ for translation). Note that counter to typical chemical physics terminology with respect to degrees of freedom, the present convention declares each nuclear coordinate containing 1/2 kT of internal energy in equilibrium to be a degree of freedom. The probability for reaction including vibrational favoring is given by:

$$P(f_v) = P^o(f_v)\exp(-\lambda f_v) = \\ A f_v^{\zeta_v - 1}(1 - f_v)^{\zeta_b - 1} \exp(-\lambda f_v) \tag{10}$$

where the gamma terms in the prior expression have been absorbed into the A factor, and

$$\lambda = \lambda_c + \lambda_T T_{rel} \tag{11}$$

13

Here, λ_c is an adjustable parameter roughly equivalent to the λ in Rebick – Levine, λ_T is a second adjustable parameter that allows the degree of favoring to vary with collision "temperature," and T_{rel} is related to the relative translational energy. Initial tests have shown that (using the suggested values for λ_T) the variability of λ due to the translational energy in the collision is a relatively small effect for the present case, so we will present comparisons using $\lambda_T = 0$ for simplicity. Thus, for the present case, the state-specific probability reduces to:

$$P(f_v) = A(1 - f_v)^{1.8} \exp(-\lambda f_v) \qquad (12)$$

for $E_c > D$; $P = 0$ otherwise. The vibrational favoring term, which has the same form as the Rebick – Levine model, suffers from the same unphysical behavior for high v levels in the case where λ is large and the collision energy is near threshold. An example is show in Figure 6(a), where dissociation probabilities for the $v = 20$ level are shown for both the ME and Rebick - Levine formulations for $\lambda = -5$ and $\lambda = -20$ cases (note the logarithmic scale). The models are quite similar here, since both are dominated by the exponential term.

The A factor is again chosen by matching the weighted sum of probabilities to the measured cross section for the cold case at $E_{tr} = 5$ eV (for each assumed value of λ) and values of $\lambda = 0$, -2, and –20 are shown in Figures 6(b-d) (note change of scale in Figure 6(d)). The values for A are 0.52, 0.5, and 0.35, respectively. Notice that for the $\lambda = 0$ case, the hot ME cross section falls below the cold ME cross section when $E_{tr} > 1$ eV. The case for $\lambda = -20$ is included because it is typical of the values recommended by Gallis and Harvey for dissociation reactions (O_2, N_2). It seems unlikely that, even assuming that O_2 and N_2 have large vibrational favoring, their cross sections for high vibrational states are increased by a factor on the order of 10,000 over the prior cross section.

Threshold Line Model

The threshold line dissociation model, due to Macheret and Rich,[38] is fully detailed in ref. 39. (A note on terminology: the term "threshold" is generally used in this paper to refer to the region where the CID cross section "turns on," just above E_a. The name of the threshold line model, on the other hand, is from the "threshold function" which determines the amount of translational energy required to dissociate a

given vibrational level in an impulsive limit.) Discussions on the DSMC implementation are given by Boyd[4] and Wadsworth and Wysong.[5] The formulae used here are those in ref. 39 as discussed by Wadsworth and Wysong. The state-specific probability expressions have a mathematical singularity for certain values of E_v. The recommended methods are employed; however, all the probability expressions become greater than one as the collision energy increases. In addition, the recommended procedure for probability expressions near the singularities (where the Taylor expansion expressions are continued to the lowest-order non-zero derivative) cause some non-monotonic increase in probability with vibrational level for most collision energies. For the present collision system the vibrational levels $v \cdot 8$ are considered "low" levels, while the levels greater than 8 are considered "high" levels. The expressions for $v = 7, 8$ and 9 are close enough to the dividing point to blow up due to that singularity, and these have had the appropriate procedure applied. The probability for $v = 10$ behaves well at low energies, but for $E_{tr} > 2$ eV it is near enough to the singularity to become spuriously high and cross the values for $v = 11\text{-}14$. Similarly, $v = 6$ behaves well at low energies, but for $E_{tr} > 2$ eV the cross sections grow rapidly with energy and cross the values for $v = 7$ and 8. The most serious problem is with the high v levels. Figure 7(a) shows the state-specific dissociation probability for very high vibrational levels as a function of translational energy. These are the levels that, with any population at all, tend to dominate the dissociation rate because they are close to D in energy. In the figure, the expressions for $v = 24, 25$ have had the procedure applied and it is evident that their behavior is radically different from the other levels. It is clear that the probability for dissociation for any vibrational level will become greater than one at some point as E_{tr} is increased in this model, and the application of the near-singularity procedures is fairly arbitrary, depending on the given level and the range of E_{tr}. Boyd[4] has also noted that the probabilities for excited vibrational levels become much greater than unity in this model. In a case where the leading constant in the model is obtained through calibration against rate coefficients, it may be argued that the occurrence of reaction probabilities greater than unity is in itself not a problem. However, this behavior is clearly not desirable in any CID model and indicates an important limitation of the threshold line model.

The probabilities for each level have been weighted by the measured populations and summed; a hard-sphere (constant) total cross section has been assumed. Figure 7(b) below shows the result where the cold case and hot cases have been normalized to match the measurement at $E_{tr} = 5$ eV using a factor of $A = 13$. It is important to note that the threshold line model is designed for cases when E_c is not much greater

than D. Previous studies[4,5] have examined state-specific thermal equilibrium rate constants for the threshold model for N_2 at 10,000K, O_2 at 10,000K and H_2 at 4500K. where a typical collision has E_{tr} about 15% of D. Thus, these cases did not probe the very high collision energies that are involved in the present data (the measured cross sections for Ar_2^+ have E_{tr} up to $3D$). Nevertheless, a previous study[5] did note a significant distortion of results due to the problem of probabilities greater than one. Figure 7(c) shows the result when we concentrate on the lower energy regime and re-normalize the threshold model cross sections to match the cold data at $E_{tr} = 3$ eV.

Total Collision Energy (TCE) Model

Bird's chemistry model[1] which reproduces given reaction rate coefficients is sometimes referred to as the total collision energy (TCE) model. This approach is by far the most widely used in DSMC codes. The reason is that, in the majority of cases, no direct cross section information is available about the reactions of interest; instead, measured rate coefficients are available for some range of temperatures, implying equilibrium conditions and equivalence of all forms of energy.

The Ar_2^+-Ar case should provide an optimal test for this model, since vibrational favoring is found to be minimal and because the above experiments provide more information than normal. In order to obtain an estimation of $k(T)$, we take an assumed functional form for $\sigma_R(v, E_{tr})$, the $\lambda = 0$ WVB / Levine (for $n = 1$) form above, where $A = 19$ Å^2 to match the measured cold cross section at $E_{tr} = 5$ eV. This σ_R is integrated over a thermal translational energy distribution to get $k(v,T)$ for each vibrational level. This assumes that rotational energy is either not present or is not contributing to the reaction cross section, consistent with the assumption that the Ar_2^+ primary ions of the experiment are rotationally cold.

The total "thermal" (quotation marks here because the assumption of no rotational energy is of course not true thermal equilibrium) rate coefficient for each temperature is:

$$k(T) = \sum_v k_v(T) N_v(T) \tag{13}$$

where $N_v(T)$ is the Boltzmann fraction of population in level v. This $k(T)$ information is fit to an Arrhenius form:

$$k(T) = A' T^\eta \exp(-E_a / kT) \tag{14}$$

16

The fit produces $A' = 9.7 \times 10^{-12}$ cm^3/s, $\eta = 0.5$, $E_a = 1.316$ eV for the temperature range 300 – 2000K. This is expected, since Levine and Bernstein[40] have shown that a $k(T)$ Arrhenius form with $\eta = 0.5$ can be inverted to give a cross section of the simple LCCS form.

Eq. 6.8 from ref. 1 is used to get reaction cross section or probability based on the VHS parameters, the Arrhenius parameters, and $\bar{\zeta}$, the average number of internal DOF that contribute to the reaction. Ar contributes no internal energy, while Ar_2^+ contributes vibrational energy (2 DOF is used for this mode, which is reasonable, since the vibration is significantly excited even in the cold case, see also Boyd[41]) and no rotational energy (by assumption), which makes an average of 1. The VHS parameters as described above are used.

Figure 8(a) shows the result; note that in this case, since there is no distinction in the model between vibrational and translational energy, the ordinate is E_c $(= E_v + E_{tr})$. For the measured data, we use the measured average vibrational energy for each distribution $E_c = E_{tr} + 0.09$ eV for the cold case and $E_c = E_{tr} + 0.77$ eV for the hot case. The figure also shows the TCE result that is obtained if one were to assume that no internal DOF contribute to the reaction probability, i.e., $\bar{\zeta} = 0$, which demonstrates that the results are quite sensitive to the value of this parameter (see also Bird,[42] Boyd,[41] Gimelshein et al.[3]).

Vibrationally Favored Dissociation Model

Haas and Boyd[8] proposed a DSMC chemistry model that is based on the TCE model and similarly reproduces given rate coefficients, but adds a vibrational favoring factor of the form $(E_v/E_c)^\phi$ to the probability expression, where $\phi = 0$ represents the TCE limit. By comparisons with shock tube data for O_2 and N_2, values of 0.5 and 2 for ϕ were suggested, respectively. Figure 8(b) shows results for the VFD model, with $\phi = 0.5$, compared with the Ar_2^+ cold and hot cross sections. As for the other models, the model cross section has been arbitrarily normalized to match the data at $E_{tr} = 5$ eV; this results in a scaling of the VFD result by a factor of 4.4.

The VFD cross sections for $\phi = 0.5$ are similar to the Rebick - Levine or WVB cross sections for the case of significant but not huge vibrational favoring. Figure 8(c) shows the result when $\phi = 2$, where a

scaling factor of 79 is used to match the cold data at $E_{tr} = 5$ eV. In this case a logarithmic scale is used, since the model cross section for the hot case reaches over 1000 A^2.

Discussion

The recently published Ar$_2^+$ + Ar CID measurements provide a unique opportunity to compare existing dissociation models with actual experimental data. Table 2 summarizes key aspects of the DSMC model comparisons for the present case. Since all the models use an adjustable scaling factor, A, it is not included in the list of parameters. In addition, although the VHS parameters occur explicitly in some of the models and not in others, the uncertainty of how to correctly simulate the total collision cross section is inherent in the implementation of any chemistry model into the DSMC technique and so these parameters are not included in the table. The comments are in relation to the present Ar$_2^+$ - Ar comparison and are obviously somewhat subjective.

One important point is the physical regime towards which the development and application of most of the DSMC models have been oriented. This regime is a shocked flow typical of hypersonic flight or re-entry through an atmosphere, where the translational "temperature" is very high but the vibrational "temperature" is much lower. While this regime is in extreme nonequilibrium, it is more similar to the case of the cold Ar$_2^+$–Ar data than to the hot data. The hot data, with its extremely high degree of vibrational excitation with respect to the dissociation energy, introduces a new regime for which these models were not originally developed. While the dynamics at low translational energies are characteristic of an expanding flow, the high translational energy dynamics of the hot Ar$_2^+$ ions have some similarities to the conditions of an expanding plume in a spacecraft or rocket that undergoes collisions with fast atmospheric species. The present comparisons highlight the potential problems in extending the models into regimes with greater vibrational excitation and the significant difficulties associated with estimating or validating adjustable parameters for CID models exclusively through comparisons with rate coefficients, $k(T)$. The temperature-dependent values for $k(T)$, whether for equilibrium or for the nonequilibrium vibrational distributions often present in shock tube measurements, are primarily governed (for CID or any highly endothermic reaction) by the large variation with temperature of the fraction of collisions that satisfy $E_c > E_a$.[5] The problem of correctly interpreting the sensitivity of $k(T)$ to an adjustable parameter in a DSMC model is exacerbated when the model predicts a probability greater than unity for any non-negligible fraction of collisions.

The Rebick - Levine and WVB models are based on hard-sphere line-of-centers energy transfer and provide cross sections rather than rate coefficients. These expressions are easily fit to experimental measurements of the energy dependence of CID cross sections. There is, however, no simple recipe for determining the parameters λ, A and n for the usual case that no experiments exist. Then, the only access to reliable values are extensive quantum chemical calculations of the potential energy surface and quasiclassical trajectory calculations using the determined surface. The problem is rendered substantially more complicated if multiple potential energy surfaces play an important role. In the present collision system, complications could arise due to the presence of a charge-transfer surface that is essentially resonant with the CID products. Multiple potential energy surfaces will also play an important role at high translational energies due the onset of nonadiabatic effects.

For the present data, the Rebick – Levine model with $n = 1.5$ provides a closer match to the shape of the measured cross sections than the WVB model ($n = 1$ is assumed). On the other hand, the WVB form may have advantages in a bounded probability expression and a more physical shape of the energy dependence of the favoring term, as discussed above. The ME model appears to have an incorrect formulation of the prior cross section (the formulation is correct, however, for the prior probability in inelastic collisions). The model displays poor near-threshold behavior, and the recommended values for λ appear highly unphysical.

The threshold-line model has the attractive feature of no adjustable parameters and is probably reasonable when limited to cases when the typical collision energy is close to D and the dissociation reaction has significant vibrational favoring. Probabilities for vibrational levels near the threshold-line and near D are problematic. The decision of when to apply the near-singularity procedure and when not to is rather arbitrary, and the procedure may change the results significantly in some cases.

In the present negligible vibrational favoring case, the TCE model provides a reasonable comparison. This model depends on the knowledge of $k(T)$ over a sufficient temperature range to obtain good Arrhenius parameters extending into the collision energy range of interest. When vibrational favoring is not considered important, the present comparisons suggest using this model. In addition to E_a (which is critically important to know for any model), the Arrhenius parameters provide η, which is what determines the shape of the cross section produced by this model and thus plays the same role that n plays in the

19

Rebick – Levine model. However, even when the above conditions are met, significant discrepancies may arise when $\bar{\zeta}$ is not known or a poor value is used.

The VFD model performs in a satisfactory manner, if one has good values for the Arrhenius parameters extending into the collision energy range of interest and for a physically viable choice of ϕ. Note that since $P(E_v = 0) = 0$, a quantized implementation of vibrational energy, $E_v = (v + 0.5)h\nu$, and a use of a dissociation energy including zero-point energy, $D + 0.5\,h\nu$, is preferred. The present study shows that $\phi = 2$ produces a very strong vibrational favoring, and the suggestion of $\phi = 3$ for some cases (Boyd[43]) gives even more extreme results. For comparison, if $E_v/D = 0.5$, the $(E_v/E_c)^2$ term gives an enhancement of probability compared with $E_v/D = 0.02$ (typical for $v = 0$) on the order of several thousand (when E_c is around $1.1D$). In contrast, the data on H_2^+, a very strongly vibrationally favored case, indicate an enhancement on the order of 10-20 for these values of E_v and E_c. The measured probability enhancement would be consistent with a Levine/Kiefer enhancement term, $\exp(-\lambda E_v/D)$, for $\lambda = -5$.

As mentioned earlier, in several models assumptions of the translational energy dependence of a total cross section are required. For the present ionic system, transport cross sections have been provided by mobility data.[32] Mobility data, however, are limited to low average translational energy (<0.2 eV) and involve an energy regime where the attractive interaction plays an important role. Meanwhile, the DSMC definition of transport cross sections being associated with isotropic scattering in the center-of-mass frame is problematic at higher translational energies, where reactive as well as non-reactive inelastic scattering can become highly anisotropic and an isotropic scattering cross section can become smaller than a dissociation cross section. This is exemplified by the highly forward-peaked fragment ion scattering observed in the present Ar_2^+–Ar CID system at high translational energies. Here, we suggest using transport data such as mobility measurements for energies at which the cross sections are larger than a hard-sphere cross section dictated by the van der Waals radii of the species involved. At higher energies, the hard-sphere cross section should be used. It is likely that the latter should increase with vibrational excitation, particularly if excitation occurs to levels where anharmonicity effects are large and the vibrating molecule spends a large fraction of time near the outer turning point of the oscillatory trajectory. However, no validated method for connecting the increased radius of the diatomic potential well to the effective transport collision cross section has yet been proposed.

The present comparison to one particular experimental study raises the question as to how generally the lessons of Ar_2^+–Ar can be applied. It is too early to state whether the negligible, if not inhibitive, effect of vibrational energy is a general phenomenon of heavy-atom diatomics or is particular to this collision system only. CID is a process that can be in direct competition with other processes. In the case of Ar_2^+–Ar, charge transfer, experimentally not distinguishable from CID, is essentially resonant with CID, and a chemical exchange channel, experimentally not distinguishable from the reactants, is coupled with CID. Both of these channels depend on the choice of target gas. To test the effect of multiple surfaces, we have conducted preliminary quasiclassical trajectory (QCT) studies on a LEPS potential energy surface that provides an optimal fit to the potential points calculated by De Lara et al.[29] The calculated CID cross sections exhibit substantial vibrational favoring corresponding to a Rebick and Levine parameter of $\lambda = -2.9$. Since the calculations include the effects of the atom-exchange channel, the discrepancy between experiment and QCT calculations hints that the charge exchange interaction, not incorporated in the calculations, may play an important role in undermining the expected vibrational enhancement.

To further pursue this lead, we are currently conducting an investigation of the Ar_2^+–Ne system, where the charge-transfer channel is highly endothermic and where $ArNe^+$ and ArNe chemical exchange products are both very weakly bound. First results, to be published with the QCT calculations,[44] indeed show a substantial vibrational enhancement for the Ar_2^+–Ne system near threshold. Finally, the role of electronically excited states near the dissociation limit, several of which exist for Ar_2^+, may also be important, and should be included in any statistical approach. An experiment is being constructed at the Lawrence Berkeley Advanced Light Source where the high-intensity synchrotron radiation will be exploited to produce beams of vibrationally and electronically state-selected ions using a novel pulsed-field ionization (PFI) technique [Principal investigators: C. Y. Ng and R. A. Dressler]. The dissociation dynamics ions, such as O_2^+, in selected high vibrational states will be investigated.

Conclusions

The CID process for Ar_2^+–Ar does not show a vibrational favoring effect. However, other evidence supports the model of vibrationally favored CID for other diatomic molecules. The lack of a vibrational enhancement in the Ar_2^+–Ar CID system may be an anomaly attributable to the interference with a near-resonant charge exchange channel. The fidelity of DSMC models of CID is hampered by a poor

understanding of the definition of the total collision cross section, especially when a wide range of collision energies is considered. Comparisons with measured or extrapolated equilibrium rate coefficients, k(T), form a necessary but far from sufficient means of validating a DSMC chemical reaction model. This is particularly true when the value of an adjustable favoring parameter is determined through comparisons with rate coefficients. The resulting values may lead to unphysical probabilities (or cross sections) as seen with some of the models discussed above. At minimum, an examination of the model probabilities over a reasonable range of the parameter space is recommended. Of course, further measurements of CID cross sections, especially for a range of vibrational levels, will be invaluable.

Acknowledgements

References

[1] G.A. Bird, *Molecular Gas Dynamics and the Direct Simulation of Gas Flows*, Clarendon Press, Oxford (1994).

[2] Boyd, I.D., Candler, G.V., and Levin, D.A., "Dissociation modeling in low density hypersonic flows of air," *Phys. Fluids*, vol. 7, 1995, pp. 1757-1763.

[3] Gimelshein, S.F., Levin, D.A., Drakes, J.A., Karabadzhak, G.F., and Ivanov, M.S., "Ultraviolet radiation modeling from high altitude plumes and comparison with Mir data," *AIAA J.*, vol. 38, 2000, pp. 2344-2352.

[4] Boyd, I.D., "A threshold line dissociation model for the direct simulation Monte Carlo method," *Phys. Fluids,* vol. 8, 1996, pp. 1293-1300.

[5] Wadsworth, D.C., and Wysong, I.J., "Vibrational favoring effect in DSMC dissociation models," *Phys. Fluids,* vol. 9, 1997, pp. 3873-3884.

[6] Koura, K., "A set of model cross sections for the Monte Carlo simulation of rarefied real gases: atom-diatom collisions," *Phys. Fluids, vol. 6,* 1994, pp. 3473-3486.

[7] Gallis, M.A., and Harvey, J.K., "Maximum entropy analysis of chemical reaction energy dependence," *J. Thermophys. Heat Transf.,* vol. 10, 1996, pp. 217-223; Gallis, M.A., and Harvey, J.K., "The modeling of chemical reactions and thermochemical nonequilibrium in particle simulation computations," *Phys. Fluids,* vol. 10, 1998, pp. 1344-1358.

[8] Haas, B.L., Boyd, I.D., "Models for direct Monte Carlo simulation of coupled vibration-dissociation," *Phys. Fluids A,* vol. 5, 1993, pp. 478-489; Boyd, I.D. in *Chemical Dynamics in Extreme Environments*, ed. R. Dressler, World Scientific Press (2000).

[9] Gimelshein, S.F., Gorbachev, Yu.E., Ivanov, M.S., and Kashkovsky, A.V., "Real gas effects on the aerodynamics of 2D concave bodies in the transitional regime," *Rarefied Gas Dynamics 19*, edited by J.K. Harvey and R.G. Lord, Oxford Press, 1995, pp. 556-563.

[10] Carlson, A.B., and Bird, G.A., "Implementation of a vibrationally linked chemical reaction model for DSMC," *Rarefied Gas Dynamics 19*, edited by J.K. Harvey and R.G. Lord, Oxford Press, 1995, pp.434-440.

[11] Lord, R.G., "Modeling vibrational energy exchange of diatomic molecules using the Morse interatomic potential," *Phys. Fluids*, vol. 10, 1998, pp. 742-746.

[12] Armentrout, P.B., "Kinetic energy dependence of ion-molecule reactions: guided ion beams and threshold measurements," Int. J. Mass Spectrom., vol. 200, 2000, pp. 219-243.

[13] Liao, C.-L., Xu, R., Flesch, G.D., Baer, M., and Ng, C.Y., "Experimental and theoretical total state-selected and state-to-state absolute cross-sections: 1. the $H_2^+(X,v')+Ar$ reaction," *J. Chem. Phys.*, vol. 93, 1990, pp. 4818-4831.

[14] Chupka, W.A., Berkowitz, J., and Russel, M.E., *Sixth International Conference on the Physics of Electronic and Atomic Collisions: Abstracts of Papers*, M. I. T. Press, Cambridge, 1969.

[15] Chiu, Y.H., Pullins, S., Levandier, D.J., and Dressler, R.A., "Collision-induced dissociation dynamics of Ar_2^+ at high levels of vibrational excitation," *J. Chem. Phys.*, vol. 112, 2000, pp. 10880-10889.

[16] Levine, R.D., and Manz, J., "Effect of reagent energy on chemical reaction rates - information theoretic analysis," *J. Chem. Phys.*. vol. 63, 1975, pp. 4280-4303.

[17] Blais, N.C., and Truhlar, D.G., "Monte Carlo trajectory study of $Ar+H_2$ collisions," *J. Chem. Phys.*, vol. 66, 1977, pp. 772-778.

[18] Martin, P.G., and Mandy, M.E., "Analytic temperature dependences for a complete set of rate coefficients for collisional excitation and dissociation of H_2 molecules by H atoms," *Astrophys. J.*, vol. 455, 1995, pp. L89-L92.

[19] Marrone, P.V., and Treanor, C.E., "Chemical relaxation with preferential dissociation from excited vibrational levels," *Phys. Fluids*, vol. 6, 1963, pp. 1215-1221.

[20] Kiefer, J.H., and Hajduk, J.C., "A vibrational bias mechanism for diatomic dissociation: induction times and steady rates for O_2, H_2, and D_2 dilute in Ar," *Chem. Phys.*, vol. 38, 1979, pp. 329-340.

[21] Sergievskaya, A.L., Kovach, E.A., Losev, S.A., and Kuznetzov, N.M., "Thermal nonequilibrium models for dissociation and chemical exchange reactions at high temperatures," AIAA Paper 96-1895, June, 1996.

[22] Esposito, F., and Capitelli, M., "Quasiclassical molecular dynamic calculations of vibrationally and rotationally state selected dissociation cross section: $N+N_2(v,j) = 3N$," *Chem. Phys. Lett.*, vol. 302, 1999, pp. 49-54; Esposito, F., Capitelli, M., and Gorse, C., "Quasi-classical dynamics and vibrational kinetics of $N+N_2(v)$ system," *Chem. Phys.*, vol. 257, 2000, pp. 193-202.

[23] Capitelli, M., Esposito, F., Kustova, E.V., and Nagnibeda, E.A., "Rate coefficients for the reaction $N_2(i)+N = 3N$: a comparison of trajectory calculations and the Treanor-Marrone model," *Chem. Phys. Lett.*, vol. 330, 2000, pp. 207-211.

[24] Mizobata, K., "An analysis of quasiclassical molecular collisions and rate processes for coupled vibration-dissociation and recombination," AIAA Paper 97-0132, Jan., 1997.

[25] Parks, E.K., Inoue, M., and Wexler, S., "Collision induced dissociation of CsI and Cs_2I_2 to ion pairs by Kr, Xe, and SF_6," *J. Chem. Phys.*, vol. 76, 1982, pp. 1357-1379.

[26] Govers, T.R., and Guyon, P.-M., "State-selected ion molecule reactions – $H_2^+(v)+He$--HeH^++H and $He+H^++H$," *Chem. Phys.*, vol. 113, 1987, pp. 425-443.

[27] Williams, S., Chiu, Y., Levandier, D.J., and Dressler, R.A., "Determination of photofragment ion translational energy and angular distributions in an octopole ion guide: A case study of the Ar_2^+ and $N_2O·H_2O^+$ cluster ions," *J. Chem. Phys.*, vol. 109, 1998, pp. 7450-7461.

[28] Signorell, R., Wüest, A., and Merkt, F., "The first adiabatic ionization potential of Ar_2," *J. Chem. Phys.*, vol. 107, 1997, pp. 10819-10822.

[29] De Lara, M.P., Villarreal, P., Delgado-Barrio, G., Miret-Artés, S., Buonomo, E., and Gianturco, F.A., "Fragmentation of Ar_3^+ clusters via vibrational predissociation," *Chem. Phys. Lett.*, vol. 242, 1995, pp. 336-342.

[30] Koura, K., and Matsumoto, H., "Variable soft sphere molecular model for inverse-power-law or Lennard-Jones potential," *Phys. Fluids A*, vol. 3, 1991, pp. 2459-2465.

[31] Nanbu, K., and Kitatani, Y., "An ion-neutral species collision model for particle simulation of glow discharge," *J. Phys. D*, vol. 28, 1995, pp. 324-330.

[32] Ellis, H.W., Pai, R.Y., McDaniel, E.W., Mason, E.A., and Viehland, L.A., *At. Data and Nucl. Data Tables vol. 17*, 1976, p. 177; Ellis, H.W., Thackston, M.G., McDaniel, E.W., and Mason, E.A., *At. Data and Nucl. Data Tables vol. 31*, 1984, p. 113.

[33] Hassan, H.A., and Hash, D.B., "A generalized hard-sphere model for Monte Carlo simulation," *Phys. Fluids A,* vol. 5, 1993, pp. 738-744.

[34] Gimelshein, S.F., Ivanov, M.S., Markelov, G.N., and Gorbachev, Yu.E., "Statistical simulation of nonequilibrium rarefied flows with quasiclassical vibrational energy transfer models," *J. Thermophys. Heat Transfer,* vol. 12, 1998, pp. 489-495.

[35] Wysong, I.J., "Molecular collision models for reacting flows: should molecular diameters which depend on internal energy state be incorporated in DSMC simulations?," *Rarefied Gas Dynamics,* vol. 2, edited R Brun et al., Cepadues Editions, Toulouse, 1999, pp. 3-14.

[36] Rebick, C., and Levine, R.D., "Collision induced dissociation: a statistical theory," *J. Chem. Phys.,* vol. 58, 1973, pp. 3942-3952.

[37] Marriott, P.M., and Harvey, J.K., "Modeling chemical reactions in nonequilibrium rarefied flows using direct simulation Monte Carlo approach," *Rarefied Gas Dynamics: Experimental Techniques and Physical Systems,* edited by B.D. Shizgal and D.P. Weaver, AIAA, Washington, DC, 1994, pp. 197-207.

[38] Macheret, S.O., and Rich, J.W., "Nonequilibrium dissociation rates behind strong shock waves: classical model," *Chem. Phys.,* vol. 174, 1993, pp. 25-43.

[39] Macheret, S.O., Fridman, A.A., Adamovich, I.V., Rich, J.W., and Treanor, C.E., "Mechanisms of nonequilibrium dissociation of diatomic molecules," AIAA Paper 94-1984, June, 1994.

[40] Levine, R.D., Bernstein, R.B., "Post-threshold energy dependence of the cross section for endoergic processes: vibrational excitation and reactive scattering," *J. Chem. Phys.,* vol. 56, 1972, pp. 2281-2287.

[41] Boyd, I.D., "Assessment of chemical nonequilibrium in rarefied hypersonic flow," AIAA paper 90-0145, Jan., 1990.

[42] Bird, G.A., "Simulation of multi-dimensional and chemically reacting flows," *Rarefied Gas Dynamics,* vol. 1, edited by R. Campargue, CEA, Paris, 1979, pp. 365-388.

[43] Boyd, I.D., "Analysis of vibration-dissociation-recombination processes behind strong shock waves of nitrogen," *Phys. Fluids A,* vol. 4, 1992, pp. 178-185.

[44] J. S. Miller, Y. H. Chiu, D. J. Levandier, R. A. Dressler and I. Wysong, in preparation.

Table 1 Energies of Notional Vibrational Levels and Population Distribution for Cold and Hot Cases

Notional Vibrational Level	Energy (eV)	Population fraction (Cold Case)	Population fraction (Hot Case)
0	0.010	0.250	0
1	0.047	0.207	0
2	0.084	0.161	0
3	0.121	0.123	0
4	0.159	0.091	0
5	0.197	0.068	0.003
6	0.235	0.060	0.011
7	0.274	0.041	0.017
8	0.328	0	0.023
9	0.373	0	0.028
10	0.420	0	0.034
11	0.468	0	0.042
12	0.517	0	0.050
13	0.567	0	0.056
14	0.619	0	0.059
15	0.672	0	0.061
16	0.699	0	0.062
17	0.782	0	0.075
18	0.839	0	0.084
19	0.898	0	0.090
20	0.957	0	0.087
21	1.018	0	0.074
22	1.081	0	0.055
23	1.145	0	0.033
24	1.210	0	0.023
25	1.276	0	0.031

Table 2 Summary of DSMC Model Comparisons

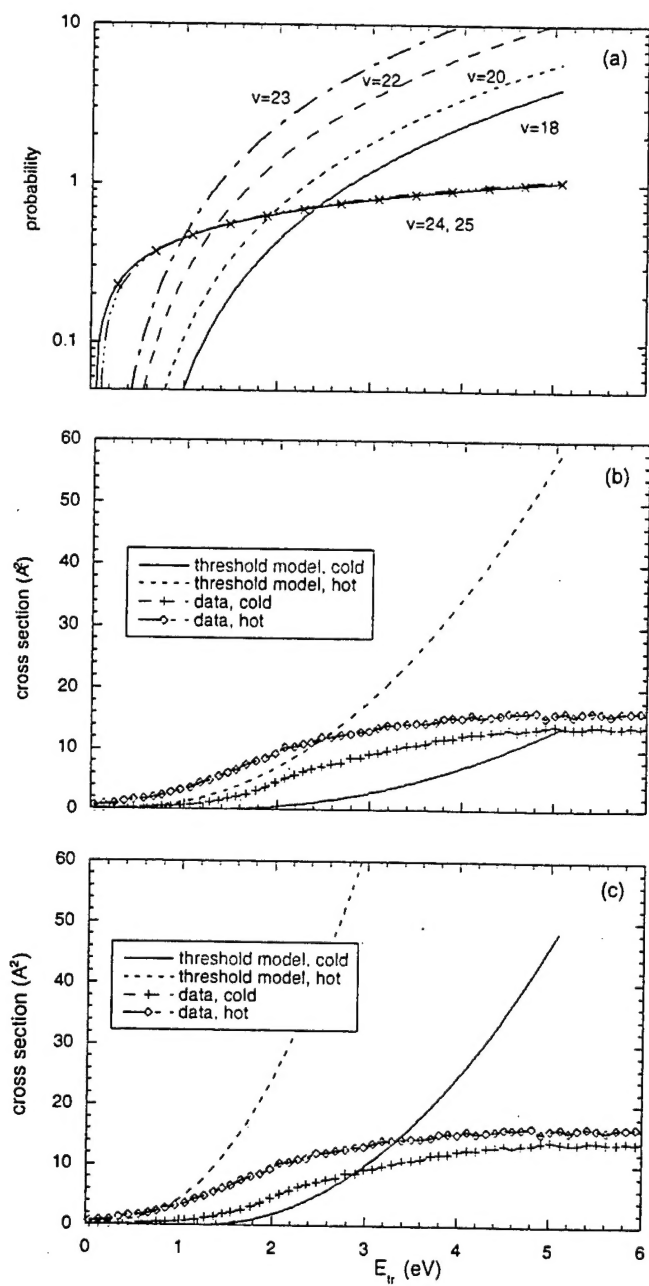| Model	Parameters to Determined	Comparison with Ar_2^+–Ar data
TCE	$\bar{\zeta}, \eta$	good
VFD	$\bar{\zeta}, \phi, \eta$	reasonable, for small ϕ
Threshold	none	poor, $P(v) > 1$ for high v
ME	λ	poor, particularly near threshold
WVB	λ	reasonable
Rebick -- Levine	n, λ	good

Figure 7. (a) CID probabilities for individual v levels for threshold-line model; (b) Threshold-line model result; (c) Threshold-line model result, renormalized
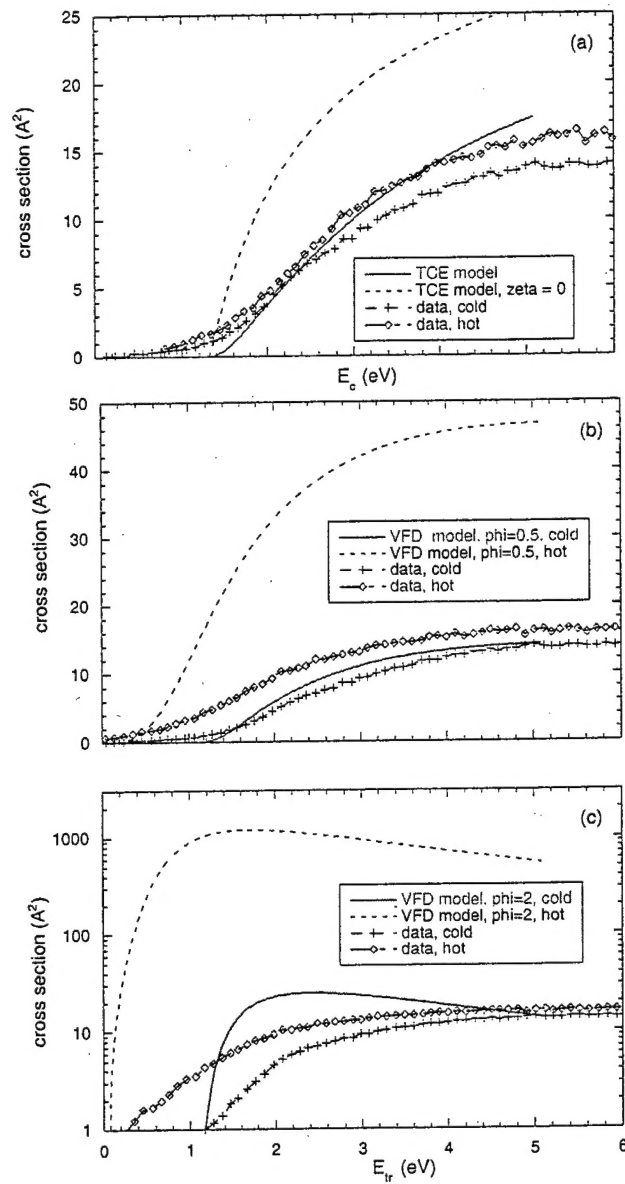
30

Figure 8. (a) TCE model result – here, the abscissa is E_c; (b) VFD model result for $\phi = 0.5$ – here, the abscissa is E_{tr}; (c) VFD model result for $\phi = 2.0$